ENVIRONMETRICS, VOL. 5, 221–239 (1994)

A SEASONAL MARKOV MODEL FOR EXTREMELY LOW TEMPERATURES

STUART G. COLES
Nottingham University, U.K.

JONATHAN A. TAWN
Department of Mathematics and Statistics, Lancaster University, Lancaster LA1 4YF, U.K.

AND

RICHARD L. SMITH
University of North Carolina, U.S.A.

SUMMARY

Time series of temperatures during periods of extreme cold display long-term seasonal variability and short-term temporal dependence. Classical approaches to extremes circumvent these issues, but in so doing cannot address questions relating to the temporal character of the process, though these issues are often the most important. In this paper a model is developed with the following features: periodic seasonal effects; consistency with asymptotic extreme value theory; Markov description of temporal dependence. Smith *et al.* studied the properties of such a model in the stationary case. Here, it is shown how such a model can be fitted to a non-stationary series, and consequently used to estimate temporal aspects of the extremal process of low temperatures which have most practical and scientific relevance.

KEY WORDS Bivariate extreme value distribution Generalized extreme value distribution Generalized Pareto distribution Markov process Temperature

1. INTRODUCTION

Recent research into statistical methodology for extremes has been driven by two broad aims. The first is to make maximal use of data which contains information about the extremal characteristics of a process; the other is to address questions of greater physical detail and relevance than classical procedures allow. Traditionally, the distribution of the maximum (or minimum) of a sequence of variables–the annual maximum, say–has been the focus for analysis. The classical approach to modelling this distribution is to fit a suitable family to an observed series of annual maximum data. The family usually used is the generalized extreme value distribution (GEV), which has distribution function

$$G(z;\mu,\sigma,\xi) = \exp\left\{-\left[1+\xi\left(\frac{z-\mu}{\sigma}\right)\right]_+^{-1/\xi}\right\}, \tag{1}$$

where $x_+ = \max(0, x)$, with location, scale and shape parameters $\mu, \sigma\ (\sigma > 0)$ and ξ, respectively. This class is justified as being the entire non-degenerate limiting distributional family of linearly

CCC 1180–4009/94/030221–19

Received 15 November 1993
Revised 1 February 1994

normalized maxima of IID variables. Restricted departures from the independence assumption, including the case of weakly mixing processes, also lead to this same limiting family.[1]

The most fundamental objection to the approach of modelling the annual maximum series is the wastefulness of data–data may have been recorded hourly, yet only the annual maximum is modelled. Another issue is that most environmental processes are seasonal, in which case the asymptotic justification for the GEV family loses some credibility. Finally, in many practical situations some extremal feature of a particular process, other than the annual maximum (or minimum), may be of greatest concern.

The example considered in this paper concerns a series of daily minimum temperatures. Individual occurrences of extremely low temperatures generally are of limited consequence. By contrast, long runs of very cold weather can be particularly hazardous in many areas of social and agricultural activity. For example, certain classes of crop are likely not to survive several days of sub-freezing temperatures. Similarly, some sections of the community are thought to be sufficiently vulnerable to prolonged spells of cold weather for the U.K. government currently to make special payments available if the daily average temperature stays below a specified level for some duration. An explicit analysis of the temporal structure within periods of extreme cold therefore is far more useful than a study of just the annual minimum temperature. Our analysis is

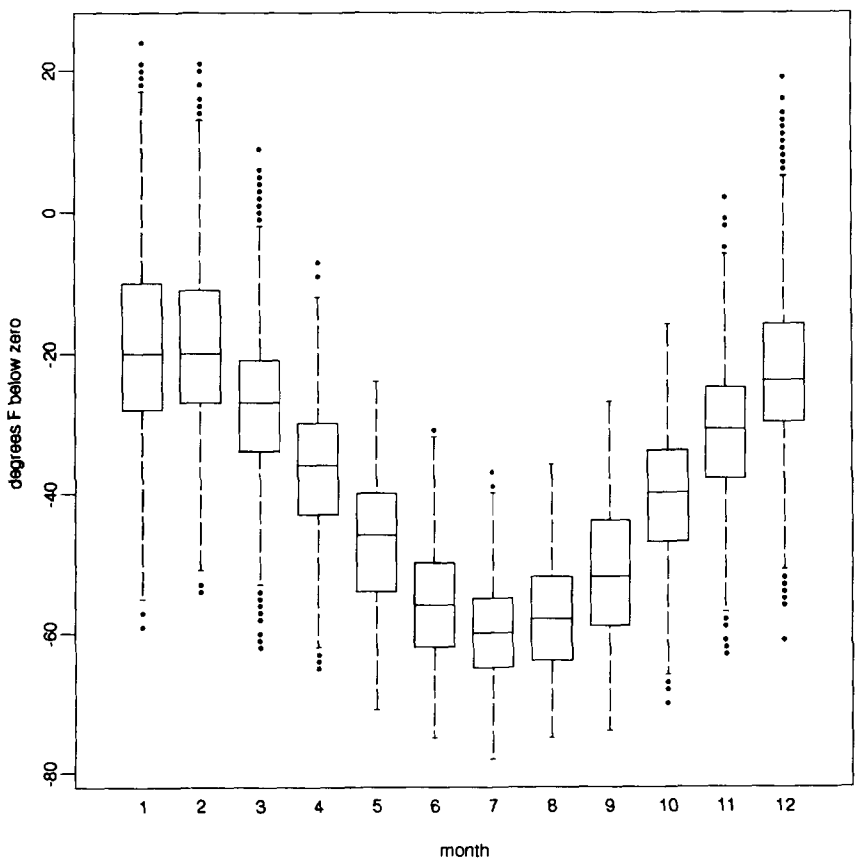

Figure 1. Monthly boxplots of the daily minimum temperatures for Wooster, Ohio

designed to allow such questions to be addressed as well as avoiding some of the deficiencies of the classical approach, such as wastefulness of data and asymptotic justification based on the inappropriate assumption of an underlying stationary series.

Our data set consists of a series of 34,518 daily minimum temperatures recorded at Wooster, northern Ohio, United States. Measurements are recorded to the nearest degree Fahrenheit. Nominally these data cover the period from June 1893 to December 1987, but there are 45 missing values. Figure 1 gives boxplots of the data by month, which shows strong seasonal variation in the series. In a companion paper, Smith *et al.*[2] analysed the data from the months December to February during which the series is reasonably stationary. In that paper a model is proposed in which the sequence of daily minima, $Y_1, Y_2, \ldots$, has the following structure:

$Y_1, Y_2, \ldots$ are taken to follow a first-order Markov process;
Each pair (Y_i, Y_{i+1}) is in the domain of attraction of a bivariate extreme value distribution.

The likelihood for this model, which is based on *all* observations that can be regarded as extreme, is easily derived and maximized numerically. Furthermore, Smith *et al.*[2] show that simulation of the fitted process at extreme levels is straightforward given certain theoretical properties of the model. Using simulated replicates from the fitted model, various characteristics of the temporal structure of the underlying process then can be estimated. The aim of this paper is to integrate the structural properties of the Markov model into a model in which seasonal variability in the extremes of the temperature series is properly accounted for. This requires some reconsideration of the modelling methodology; in particular, it is convenient to exploit a point process representation of the extremal process to model the seasonal variation. Furthermore, the specification and solution of questions concerning temporal issues require greater care than in the stationary case.

Our modelling framework permits the exploitation of limiting characterisations for the extreme tails of probability distributions.[2] In the terminology of Cox,[3] these models are

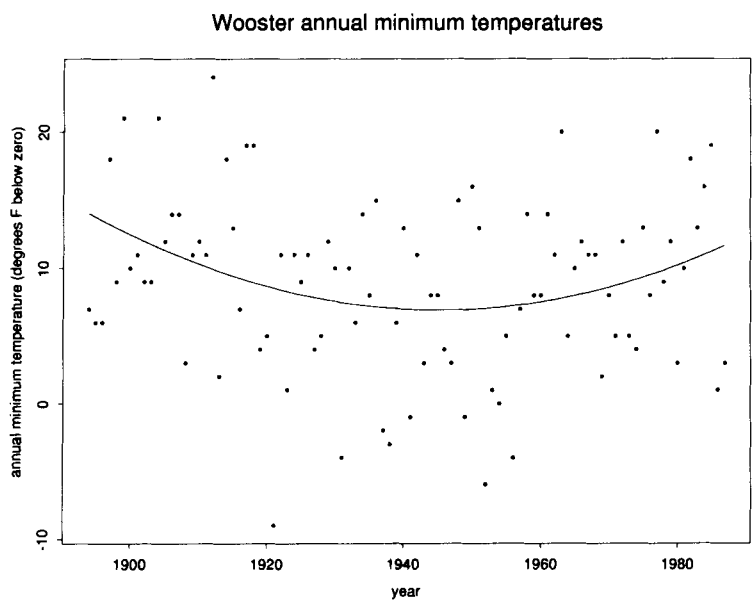

Figure 2. Annual minimum daily temperatures for Wooster, Ohio. The superimposed curve is the median of the annual minimum distribution based on the fitted GEV model

observation driven rather than parameter driven; dependence is explicitly modelled through conditional distributions rather than latent processes. Although each type of model may fit the data equally well, the justification for our approach is the desire to obtain models which have a theoretical basis for extrapolation to rare events of interest.

2. PRELIMINARY DATA ANALYSIS

For exploratory purposes, we first consider fitting the GEV model (1) to the negated series of annual minimum temperatures $\{Z_i\}$. The purpose of negating the series is to switch attention to high values rather than low, so that models based on asymptotic behaviour of maxima apply. A time series plot of $\{Z_i\}$ is shown in Figure 2. Maximum likelihood estimation of the GEV distribution yields parameter estimates $\hat{\mu} = 5{\cdot}54$ (standard error 0·73), $\hat{\sigma} = 6{\cdot}46$ (0·48) and $\hat{\xi} = -0{\cdot}33$ (0·06). However, closer inspection of Figure 2 suggests a non-linear trend. One way to deal with trends in extreme value data is to write $\mu = \mu(t) = \sum_{j=0}^{p} \beta_j t^j$ to represent an additive pth-order polynomial in time t. When this is applied to the data in Figure 2, with $p = 2$, a significant result is found (deviance 8·6 with 2 d.f.). The fitted median function $(\hat{\mu}(t) - \hat{\sigma}[1 - (\log 2)^{-\hat{\xi}}]/\hat{\xi})$ is superimposed on Figure 2. The other parameter estimates are $\hat{\sigma} = 6{\cdot}37$ (0·51) and $\hat{\xi} = -0{\cdot}34$ (0·06), so are very little changed from the first analysis.

Since the physical explanation of the trend is unclear, and the apparent effect on the other parameters very slight, in the following analysis we have chosen to ignore the trend. The focus in the present paper is on the detailed structure of the process within a cold period, and this seems unlikely to be affected by the overall trend, however caused.

3. THE STATIONARY EXTREMAL MARKOV MODEL

Our real aim is to model the extremal characteristics of the complete temperature series, giving explicit attention to the issues of short-term temporal dependence and long-term seasonal variability. It is simplest first to tackle these issues separately. Let $\{Y_i\}$ be the negated series of daily minimum temperatures. We now make two assumptions:

1. The series is first-order Markov;
2. The series is stationary, having common distribution function F.

The second of these assumptions is subsequently dropped in Section 4. Under the two assumptions the joint density of the series decomposes naturally as

$$f(y_1, \ldots, y_n) = \frac{\prod_{i=2}^{n} f(y_{i-1}, y_i)}{\prod_{i=2}^{n-1} f(y_i)}, \tag{2}$$

where f is used generically to denote joint and marginal densities. The exact form of this likelihood clearly depends on the precise form of the marginal and bivariate densities. This is undesirable since we have no interest in modelling the bulk of either the marginal or joint distributions; our interest is confined to the tails only. A sensible scheme therefore is to specify models only for the marginal and joint tails and censor the likelihood for observations which fall short of the tail area. Furthermore, conventional extreme value asymptotic arguments can be applied to suggest appropriate models for the tail behaviour. This is the approach developed by Smith *et al.*,[2] who give a thorough exposition of the model. Here we confine ourselves to a brief description only of the model.

First consider the marginal density $f(y)$. Conditional on Y exceeding a high threshold u, an approximate distribution for the excess $X = (Y - u)$ is taken as the generalized Pareto distribution (GPD). This has distribution function

$$F_u(x; \sigma^*, \xi^*) = 1 - (1 + \xi^* x/\sigma^*)_+^{-1/\xi^*}, \tag{3}$$

where σ^* and ξ^* are scale and shape parameters, respectively. This model is compatible with the annual maximum distribution having GEV form. Moreover, the parameters of the GPD, together with a parameter λ, corresponding to the exceedance rate of the threshold u, can be re-parameterized explicitly in terms of μ, σ and ξ, the GEV parameters of the corresponding annual maximum distribution, $G(z)$, in which the occurrence times of extreme observations are assumed independent. In this case

$$\begin{aligned} \sigma^* &= \sigma + \xi(\mu - u) \\ \xi^* &= \xi \\ \lambda &= 1 - \exp\left\{-N^{-1}\left[1 + \xi\left(\frac{u-\mu}{\sigma}\right)\right]^{-1/\xi}\right\}, \end{aligned} \tag{4}$$

where N is the number of observations per year. If there is some temporal dependence in the extremes, so that there is clustering of the process at high levels, then the distribution of the annual maximum becomes $G^\theta(z)$, where θ, termed the extremal index, satisfies $0 \leqslant \theta \leqslant 1$. Leadbetter[4] showed that θ^{-1} is the limit, as the threshold u increases, of the mean number of exceedances in a period during which u is exceeded. This definition can be made more rigorous, but for present purposes an intuitive notion of θ^{-1} as the mean length of extremely cold periods will suffice. Thus, θ is a key summary parameter of the temporal nature of the extremes of the process. In practice θ is unknown; we show in Section 6 how θ can be estimated from the fitted model.

Our next assumption is that the joint density $f(y_1, y_2)$ is in the domain of attraction of a bivariate extreme value distribution. This is not particularly restrictive and is a bivariate equivalent of assuming the normalized maxima of IID samples from F converge to a GEV distribution. All such bivariate limiting distributions can be represented in the form

$$G(z_1, z_2) = \exp\{-V(\tilde{z}_1, \tilde{z}_2)\}$$

where $\tilde{z}_j = \{1 + \xi_j(z_j - \mu_j)/\sigma_j\}^{1/\xi_j}; j = 1, 2$, μ_j, σ_j and ξ_j are the respective GEV parameters and V is a homogeneous function of order -1.

There are a number of parametric families available for the function V which determines the dependence structure of the joint excess distribution, and hence in the context of this paper, the temporal dependence structure through the Markov model. Our results are presented only for the best-fitting model, which is the logistic model. This is specified by

$$V(x, y) = (x^{-1/\alpha} + y^{-1/\alpha})^\alpha$$

where $0 \leqslant \alpha \leqslant 1$. The parameter α determines the strength of dependence with the limits 0 and 1 corresponding to perfect dependence and independence, respectively. Under this assumption Smith *et al.*[2] show that the joint distribution of the excesses $(X_{i,1}, X_{i,2}) = (Y_{i,1} - u_1, Y_{i,2} - u_2)$ is approximately

$$F(x_1, x_2) = 1 - V\left[\lambda_1^{-1}\{1 + \xi_1^* x_1/\sigma_1^*\}_+^{1/\xi_1^*}, \lambda_2^{-1}\{1 + \xi_2^* x_2/\sigma_2^*\}_+^{1/\xi_2^*}\right], \tag{5}$$

for suitably high thresholds u_1, and u_2, where σ_j^*, ξ_j^* and λ_j are the GPD parameters and

exceedance rate corresponding to the marginal excess distribution of the $X_{i,j}$. Derivatives of the terms (3) and (5) are substituted directly into the likelihood (2) when both $x_i > 0$ and $x_{i+1} > 0$. In other situations, the appropriate likelihood terms are censored at the threshold value u so as to avoid making distributional assumptions at levels where the asymptotic approximation is not tenable.

The point of this framework is that the likelihood is confined to modelling the extremes of the series; the model can be justified using standard asymptotic arguments, and the parameters of the model explicitly relate to the distribution of the annual maximum and the pairwise dependence of successive extreme observations. Maximizing the likelihood (2) therefore gives estimates of the parameters which determine the extremal behaviour of the process. The usefulness of such a model depends on whether it can be used to address the questions of specific temporal detail which we wish to answer. For example, it is possible to use this model to evaluate the expected length of a severely cold period, i.e. θ^{-1}, or the distribution of the aggregate of sub-freezing temperatures during cold spells, or the distribution of the annual minimum temperature. Smith *et al.*[2] demonstrate that the Markov structure with extreme value bivariate dependence has a convenient format to facilitate such calculations. This observation hinges on a result in Smith[5] which shows that, under this model, the asymptotic behaviour of the process in the tails is associated with that of a random walk, whose distribution is determined by that of the extremal bivariate model. This gives a strategy for simulating from the model; Smith *et al.*[2] give complete details of the necessary computations for this. From sample paths of extreme events simulated by this scheme, the distribution of a variety of temporal characteristics of the series can be obtained.

Some limited properties can also be evaluated analytically, without recourse to simulation. The most interesting example of this type is the extremal index, θ. Smith[5] gives an analytical expression for θ based on the Markov property, which depends only on the assumed limiting bivariate dependence model.

4. THE SEASONAL MODEL

As observed in Section 1, except over very limited periods of the year, the process of daily minimum temperatures exhibits strong seasonal variability, not least of all in the tails. We now seek to build seasonal variability into the extremal Markov model of Section 3. This is easily achieved by allowing the model parameters – μ, σ and ξ marginally, together with any dependence parameters, α – to be seasonally varying. One approach is to factorize the likelihood (2) across seasonal blocks, months say, and allow different parameters in each season. This type of approach, but without a model for the temporal dependence, is adopted by Smith[6] for studying a time series of extreme ozone levels, and also by Barrett[7] in a seasonal analysis of extreme river flows. An alternative approach is to use continuous-time periodic parametric models for $(\mu, \sigma, \xi, \alpha)$. There are a number of advantages to this approach provided a suitable model can be found: the arbitrariness of seasonal blocking is avoided; variation is measured naturally on a continuous scale; and models are more likely to be parsimonious.

Thus we take $\mu(t)$, $\sigma(t)$, $\xi(t)$ and $\alpha(t)$ to be periodic models on the interval [0,1], expressed in terms of a vector of hyperparameters, where t indexes the time of the observation in the annual cycle. However complex these models are, at any time point, t_0, the parameters $\mu(t_0)$, $\sigma(t_0)$ and $\xi(t_0)$ admit a simple interpretation: they are the GEV parameters which would apply for the annual maximum distribution of an IID process whose marginal characteristics match those observed at time t_0 in the annual cycle. A particular consequence of this is that the parameters are independent of the thresholds specified. Thus it is possible to allow the thresholds to vary throughout the year, without affecting parameter interpretation; this could not be achieved if we

Table I. Thresholds (u) and number of exceedances (n_u) for each month. Also given are the corresponding estimates of the mean cluster size (θ^{-1}) with standard errors (s.e. (θ^{-1}))

Month	u	n_u	θ^{-1}	s.e. (θ^{-1})
Jan	5·5	105	1·61	0·18
Feb	4·5	105	1·58	0·18
Mar	−9·5	118	2·18	0·29
Apr	−22·5	126	2·32	0·35
May	−31·5	137	1·64	0·19
Jun	−40·5	106	1·57	0·18
Jul	−46·5	130	1·52	0·17
Aug	−44·5	137	1·46	0·13
Sep	−34·5	103	1·44	0·15
Oct	−25·5	110	1·63	0·21
Nov	−16·5	109	2·40	0·37
Dec	0·5	104	1·65	0·18

used the usual GPD parametrization. Seasonally varying thresholds also make physical sense; what would be regarded as an extremely cold day in July is not likely to be severe by January's standards (see Figure 1). The only considerations to make in specifying the thresholds are the usual ones, choosing thresholds which give as many exceedances as possible but which are high enough for the asymptotic model to be a good approximation within each month. Another feature of modelling the GEV parameters with continuous-time covariate models is that equation (4) immediately gives a seasonal model, $\lambda(t)$, for the threshold exceedance rate.

Seasonal models are easily incorporated into the likelihood (2) by replacing the constant parameters $(\mu, \sigma, \xi, \alpha)$ with their functional forms. Numerical maximum likelihood is used to estimate the models, with standard likelihood ratio tests and supplementary diagnostics to discriminate between models. Subsequently, estimation of extremal temporal characteristics can proceed in much the same way as the stationary case, by the simulation of extremes from the fitted process.

5. THE FITTED MODEL

To obtain some idea of the seasonal structure of the extremes our first exploratory model consists of separate GEV and dependence parameters fitted within each monthly block. The model specified for the bivariate dependence corresponds to a logistic bivariate extreme value limit model. As in Smith *et al.*,[2] alternative choices for this component of the model structure were found not to result in any improvement. Also, as discussed in Section 4, parameter interpretation is not affected by threshold choice, except in so much as the asymptotic support for the model is valid only at sufficiently high levels. A sensible scheme therefore is to determine separate thresholds for each month such that there are approximately the same number of exceedances per month. This effectively assumes that the rate of convergence to the asymptotic model is the same in each month. This selection of thresholds is then adopted for each of the subsequent models. Ties in the data prevent us obtaining thresholds which give exactly the same number of exceedances per month; the values given in Table I were selected so as to obtain at least 100 exceedances per month. A number of diagnostic checks are available for the marginal exceedance component of the model,[8] and these are found to be satisfied at the specified levels. More generally, threshold validity for the whole model can be verified by exploiting the fact that the model should be independent of threshold choice once the threshold is sufficiently high. Thus, our

Table II. Likelihood comparison of fitted models. The models highlighted by an asterisk correspond to using a parametric model of the same structure as given by the model in equation (6). All other models are either separate months or Fourier representations, with the distinction being clear from the associated number of parameters

Model number	Number of parameters					NLLH
	$\mu(t)$	$\sigma(t)$	$\xi(t)$	$\alpha(t)$	total	
1	12	12	12	12	48	8072·0
2	12	1	1	1	15	8142·9
3	3	12	12	12	39	7870·4
4	3	7	7	12	29	7872·6
5	3	7	7	5	22	7885·7
6	3	7	7	*7	24	7874·3
7	3	7	7	*5	22	7876·3
8	3	*7	*7	*5	22	7873·4

approach is to fit the basic likelihood (2) separately within each month across a range of threshold choices, and adopt levels at which reasonable stability in the fitted models is observed. This validated the choices in Table I. The monthly values of the GEV parameters, μ, σ and ξ indicate that the seasonal variation in each parameter is essentially smooth, which suggests it may be possible to adopt functional forms for the parameter variation.

Let the vector of time dependent parameters $\{u(t), \sigma(t), \xi(t), \alpha(t)\}$ be denoted by $\{\psi^{(i)}(t), i = 1, \ldots, 4\}$. Then, for each $\psi^{(i)}(t)$ function, we consider modelling the time dependence initially in either of two ways:

(i) a separate months model, i.e.

$$\psi^{(i)}(t) = \psi^{(i)}_{j(t)},$$

where $j(t)$ is an index variable corresponding to the month during which time t occurs. Thus $\psi^{(i)}(t)$ has 12 parameters under this model.

(ii) a Fourier representation, i.e.

$$\psi^{(i)}(t) = c_0^{(i)} + \sum_{j=1}^{p^{(i)}} \{c_{1,j}^{(i)} \cos(2\pi jt) + c_{2,j}^{(i)} \sin(2\pi jt)\},$$

where $p^{(i)}$ is the number of Fourier frequencies in the model, and $c_{1,j}^{(i)}$ and $c_{2,j}^{(i)}$ are the amplitudes for the jth Fourier frequency. Thus $\psi^{(i)}(t)$ has $2p^{(i)} + 1$ parameters under this model.

Using combinations of these models for the individual parameters, we tried an extensive range of models, five of which (models 1–5) are given in Table II. Model 1 is the 'separate months' model referred to above. Model 2 is homogeneous in all but the location parameter. It is worth noting that a completely homogeneous model is inappropriate, since this would amount to a constant exceedance rate at common thresholds; clearly the data do not support such a model. Model 3 is a 'separate months' model in all parameters, except for the location parameter model which is sinusoidal. Model 4 also has a 'separate months' model for the dependence parameter, $\alpha(t)$, and a sinusoid for $\mu(t)$, but constrains both the scale and shape parameters to be Fourier representations. Model 5 is similar to model 4 but with a Fourier model for the dependence parameter. Models 6–8, in Table II, will be explained later.

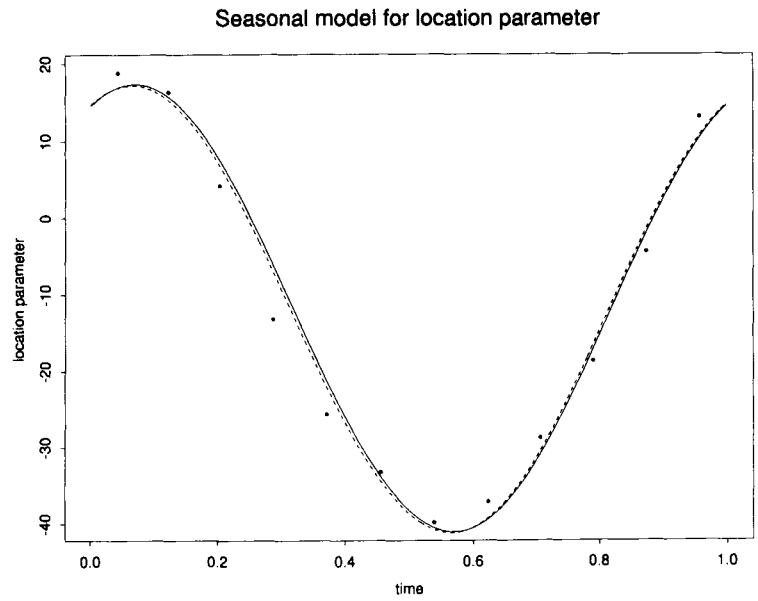

Figure 3. Location parameter, $\mu(t)$, of the generalized extreme value distribution plotted against time, t, measured on the annual cycle. The points correspond to monthly based estimates from model 1, and the continuous and dashed curves are the fitted sinusoidal model of models 7 and 8, respectively

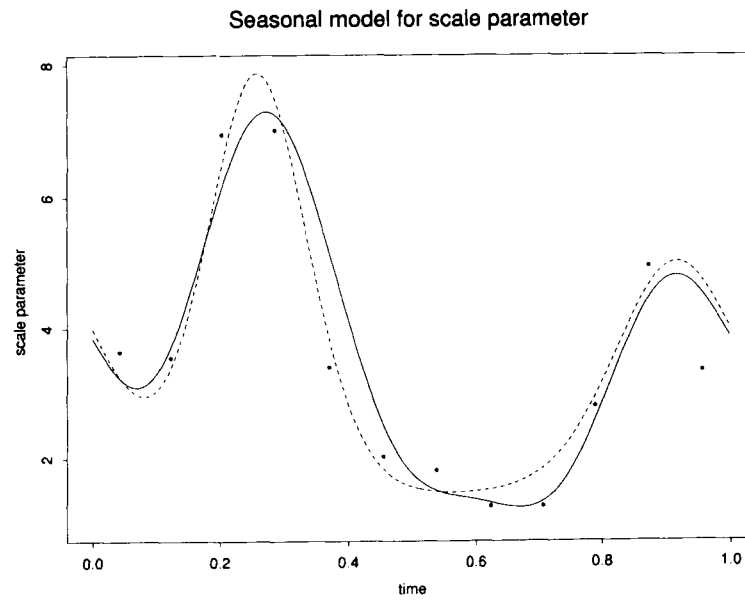

Figure 4. Scale parameters, $\sigma(t)$, of the generalized extreme value distribution plotted against time, t. The points correspond to monthly based estimates from model 3, and the continuous and dashed curves are the fitted models 7 and 8, respectively

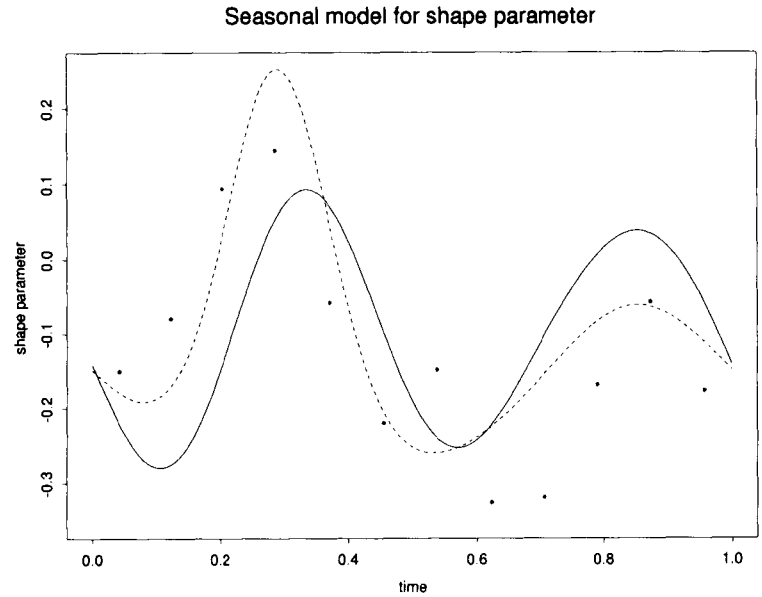

Figure 5. Shape parameter, $\xi(t)$, of the generalized extreme value distribution plotted against time, t. The points correspond to monthly based estimates from model 3, and the continuous and dashed curves are the fitted models 7 and 8, respectively

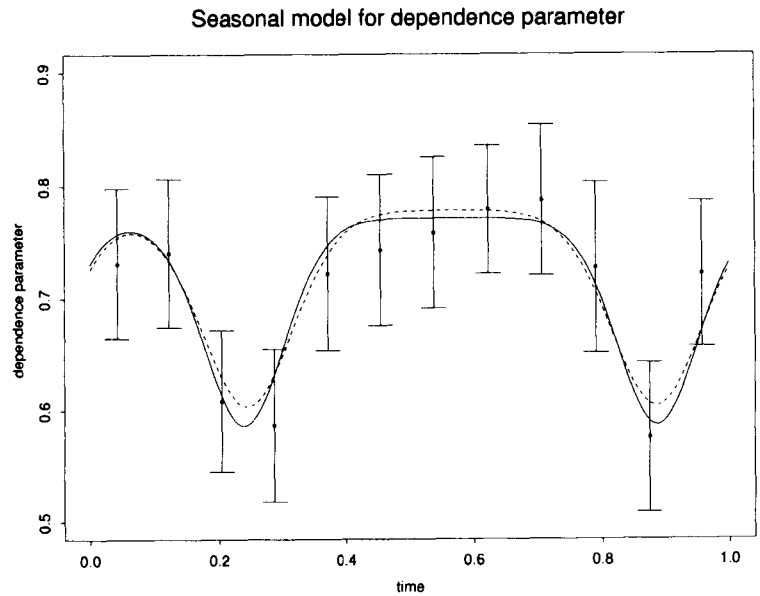

Figure 6. The logistic model dependence parameter, $\alpha(t)$, plotted against time, t. The points correspond to monthly based estimates from model 4, these are shown with associated 95 per cent confidence intervals. The continuous and dashed curves are the fitted models 7 and 8, respectively

A summary of the likelihoods obtained for each of these models is given in Table II. Figure 3 shows $\mu(t)$ estimated by use of model 1. It is clear that there is considerable seasonal variation in this parameter, but it is important to test whether the other parameters can be taken to be homogeneous over time. However, from a comparison of the likelihoods of models 1 and 2 it is immediately apparent that model 2 is hopelessly inadequate. Thus we need to model seasonal variability in all four parameters. As each of the four parameters is estimated with different levels of precision, the modelling strategy we adopt is to develop a model first for the parameter which can be estimated with greatest precision and exhibits the smoothest temporal variation, this being $\mu(t)$, then to constrain $\mu(t)$ to be in this family and simultaneously estimate models for the highly interrelated parameters $\sigma(t)$ and $\xi(t)$. The final stage, after models for the GEV parameters have been selected, is the estimation of models for $\alpha(t)$. This approach aids the identification of suitable models for the more complex shape and dependence parameters.

Model 3 fits substantially better than model 1. Although this model is simple for the location parameter, no additional Fourier terms were found to significantly improve the fit. In fact the negative log-likelihood (NLLH) for this model is lower than that of the separate monthly parameters model, despite the model having fewer parameters. This is a result of using a location parameter model which is a continuous function of time, which therefore can account for intra-month variation in the process; this feature is particularly evident in the spring and autumn months. Thus, even with this simple model we have substantial support for the use of continuous-time models in preference to models based on separate seasonal blocks.

Figures 4 and 5 show the scale and shape parameters as estimated using model 3. In each case there is evidence of a smooth seasonal variation, but with greater complexity than the simple sinusoidal form found for $\mu(t)$, suggesting the use of higher order Fourier representations. Comparison of likelihoods for models 3 and 4 suggest that these Fourier models capture the observed variability of these parameters. It is interesting to note that models with parameter configurations 3, 7, 12, 12 and 3, 12, 7, 12 each give NLLH values less than that for model 3, again suggesting there is evidence of significant intra-month variation in scale and shape parameters, respectively.

Finally, we consider the dependence parameter, $\alpha(t)$. Monthly estimates, with associated 95 per cent confidence intervals, obtained using model 4 are shown in Figure 6. There is a clear seasonal structure with a reduction in $\alpha_{j(t)}$ values, corresponding to increased temporal dependence, in the spring and autumn months. However, despite the observed variation, the best fitting Fourier representation (model 5) gives a significantly worse fit than the 'separate months' model (model 4). Thus with our initial choice of model structures, model 4 is the best fitting.

The remaining undesirable aspect of our selected model is that while it is based on continuous time models for the marginal parameters, it still has separate dependence parameters within each month. Since we have found that the standard Fourier representation model will not adequately capture the variation observed in Figure 6, to obtain a fully time-continuous model we need to construct an alternative parametric family for $\alpha(t)$. A possible climatological explanation for the temporal variation of $\alpha(t)$ is as follows. During the spring and autumn periods violent swings in temperature occur from winter to summer and vice versa. This can result in days of sub-freezing temperatures sandwiched by days in the 70–80°F range. This phenomenon has most influence on the shape of the tail of the distribution, as is evident from Figure 5. During these months, the length of an extremely cold spell can be anything up to a week. Relative to the thresholds for these months there is a consequent tendency to observe clusters of extremes with greater length than in other months. In other words, the cold spells in these transitional periods represent much colder conditions, relative to the background, than the other months, and have a tendency to be more persistent.

Based on this argument, we propose a model of the form

$$\alpha(t) = \alpha_0 - \sum_{i=1}^{2} d_i \exp\{\kappa_i[\cos(2\pi t - s_i) - 1]\} \quad \text{with} \quad s_1 < s_2 \tag{6}$$

which has seven parameters. Here, α_0 is a base level of dependence, the level which would hold throughout the year but for the existence of rapid transitional changes in seasonal temperature, s_i is the time in the year of the ith seasonal transition, d_i is the increase in dependence at the ith transitional time and κ_i is a measure of the dispersion effects, i.e. how rapid, the ith transition is. Thus the model in (6) has parameters describing all the features identified in the climatological explanation. Therefore, the only arbitrary component of the model in (6) is the form of the decay in the dependence form – we use a Von-Mises form due to the required periodicity of the model, but in principle any form of periodic decay could be used here.

Models 6 and 7 combine the previously selected models for the GEV parameters with the dependence model (6). Comparison of the likelihoods of models 4 and 6 shows the time-continuous dependence model is a good fit. Furthermore, comparison of model 6 with model 7 (where $\kappa_1 = \kappa_2$ and $d_1 = d_2$, so that the characteristics of the two transitional periods are identical in terms of dependence) suggests that the simpler model is adequate.

Model 7 therefore is adopted as our model. The objective of obtaining a parsimonious, continuous-time, seasonally varying model within the extremal-Markov framework of Smith *et al.*[2] is judged to have been met. The model has 26 fewer parameters than the standard 'separate months' model yet has a likelihood which is a reduction of nearly 200 in terms of NLLH. In summary, a complete description of model 7 is:

$$\begin{aligned}
\mu(t) &= -11{\cdot}882 + 29{\cdot}171\cos(2\pi t - 0{\cdot}437)\\
\sigma(t) &= 3{\cdot}637 + 0{\cdot}847\cos(2\pi t) + 1{\cdot}871\sin(2\pi t) - 0{\cdot}833\cos(4\pi t) - 1{\cdot}110\sin(4\pi t)\\
&\quad + 0{\cdot}193\cos(6\pi t) - 0{\cdot}805\sin(6\pi t)\\
\xi(t) &= -0{\cdot}0989 - 0{\cdot}0029\cos(2\pi t) + 0{\cdot}152\sin(2\pi t) - 0{\cdot}0673\cos(4\pi t) - 0{\cdot}149\sin(4\pi t)\\
&\quad + 0{\cdot}0276\cos(6\pi t) - 0{\cdot}008\sin(6\pi t)\\
\alpha(t) &= 0{\cdot}771 - 0{\cdot}185(\exp\{6{\cdot}354[\cos(2\pi t - 1{\cdot}507) - 1]\} + \exp\{6{\cdot}354[\cos(2\pi t - 5{\cdot}571) - 1]\}).
\end{aligned}$$

Each of these fitted functions are superimposed on the respective monthly fits in Figures 3–6. These confirm that the seasonal variation in the parameters is adequately captured by model 7, possibly with the exception of the shape parameter. The structure of this covariate model is also found to be robust to threshold choice, whilst the replacement of the logistic model with various alternatives to describe the pairwise temporal dependence did not lead to improved models.

As a final assessment of the fit of model 7, in Figure 7 we compare the estimated quantiles, $q(t)$, where

$$q(t) = \mu(t) - \sigma(t)\left\{1 - [-\log(1-p)]^{-\xi(t)}\right\}/\xi(t),$$

for models 1, 3 and 7 using exceedance probabilities $p = 0{\cdot}1, 0{\cdot}02, 0{\cdot}01$. For most months models 1 and 3 are in good agreement. Notable exceptions are the spring months (March–May), so these are the months where modelling intra-month variability is most important. The fitted quantiles from model 7 generally provide a reasonable fit but the lack of fit in March and May is slightly disturbing.

Our concern about the quality of the fit of model 7, as shown by Figures 5 and 7, forces us to reassess our model selection. As pointed out earlier, our physical argument to justify the

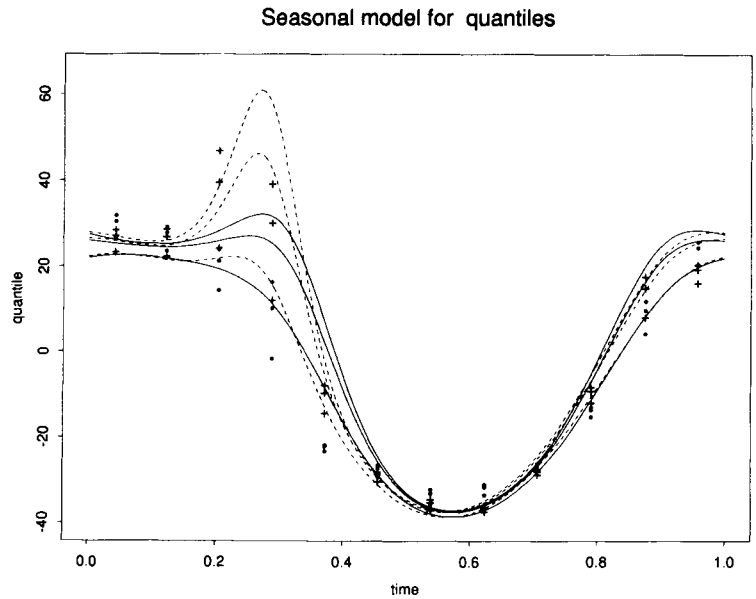

Figure 7. The quantiles, $q(t)$, of the generalized extreme value distribution function plotted against time, t. The dots and crosses correspond to estimates from models 1 and 3, respectively. The continuous and dashed curves are obtained using the fitted models 7 and 8, respectively

structural form (6) for the dependence parameter also applied to the tail parameters $\sigma(t)$ and $\xi(t)$. Thus as a final model, model 8, we consider a form which has $\mu(t)$ as a sinusoid, and $\sigma(t)$, $\xi(t)$ and $\alpha(t)$ all having the physically motivated form (6). Model 8 has an improved likelihood by comparison to model 7 despite having the same number of parameters. As models 7 and 8 are non-nested our assessment of fit is based on its properties relative the separate seasons model as well as the likelihood value. A complete description of model 8 is

$$\begin{aligned}
\mu(t) &= -12{\cdot}025 + 29{\cdot}146\cos(2\pi t - 0{\cdot}411)\\
\sigma(t) &= 1{\cdot}408 + 6{\cdot}407\exp\{4{\cdot}181[\cos(2\pi t - 1{\cdot}635) - 1]\}\\
&\quad + 3{\cdot}583\exp\{2{\cdot}776[\cos(2\pi t - 5{\cdot}768) - 1]\}.\\
\xi(t) &= -0{\cdot}344 + 0{\cdot}554\exp\{3{\cdot}746[\cos(2\pi t - 1{\cdot}834) - 1]\}\\
&\quad + 0{\cdot}282\exp\{0{\cdot}997[\cos(2\pi t - 5{\cdot}366) - 1]\}.\\
\alpha(t) &= 0{\cdot}778 - 0{\cdot}174(\exp\{4{\cdot}991[\cos(2\pi t - 1{\cdot}539) - 1]\}\\
&\quad + \exp\{4{\cdot}991[\cos(2\pi t - 5{\cdot}563) - 1]\}).
\end{aligned}$$

Each of these functions, together with $q(t)$, are plotted on Figures 3–7. Only for $\xi(t)$, and consequently $q(t)$, do these fitted forms differ much from model 7. Clearly, model 8 captures the separate seasonal features better than model 7 and has some physical justification, but this is at the cost of a non-standard functional dependence on time. Therefore, although we believe model 8 provides a more accurate description of the seasonal characteristics, both models are retained for subsequent calculations.

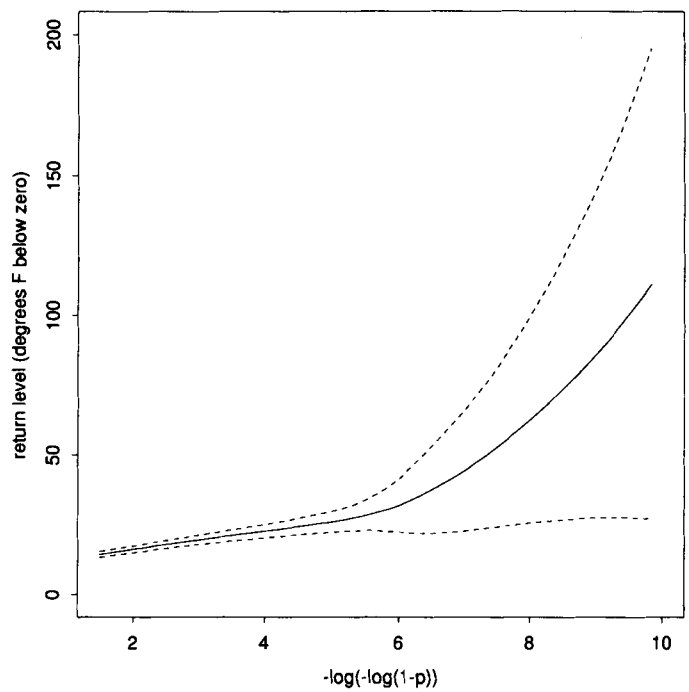

Figure 8. Return levels, y_p, of the annual minimum (continuous curve) and 95 per cent confidence intervals (dashed lines) obtained by the delta method. Estimates obtained using model 7

Before moving on to illustrating the use of these fitted models in addressing practical questions, it is helpful to compare our model with alternative models arising from analyses of these data. The seasonal pattern of both models 7 and 8 during the winter months December to February is reasonably stationary, supporting the view in Smith *et al.*[2] that this period can be modelled as a stationary series. Furthermore, the pattern of non-stationarity which can be observed over winter is similar to that identified in an empirical study of a different temperature series by Barnett and Lewis.[9] Also, by comparison with the GEV model for annual minima discussed in Section 2, the magnitude of the shape parameter $\xi(t)$ is relatively high, corresponding to heavier tail weight. However, the fitted values are more consistent with the separate monthly values than the annual minimum estimate. A possible explanation of this discrepancy is the effects of tail-mixing induced by the non-allowance for seasonality in the annual minimum approach, since from Figure 7 it is clear that December–April provides the most extreme levels, yet Figure 5 shows the tail behaviour is at its most variable within this period.

6. ESTIMATING TEMPORAL CHARACTERISTICS FROM THE FITTED MODEL

Having fitted models to describe the seasonal variability in the time-dependent series of extremely low temperatures, we now illustrate how the fitted models can be used to address a variety of questions concerning the detailed temporal behaviour of extremes of the process. For stationary series these aspects can, in principle, be assessed empirically, through empirical estimators are often highly unstable. For non-stationary series empirical approaches are less satisfactory. Our model-based approach is to simulate extreme events from the fitted model. The empirical

distribution function of, say, the simulated cluster sizes then serves as an estimator of the true cluster size distribution. Furthermore, a consequence of Theorem 1 of Smith *et al.*[2] is that the distribution of within-cluster characteristics (aggregate excesses, for example) can be convolved with a Poisson process of cluster arrivals to obtain, for example, the annual maximum aggregate distribution. In the case of a stationary extremal-Markov model, details of how to simulate from the process are given in Smith *et al.*[2] This procedure is easily modified to account for non-stationarity by parameter transformation. We illustrate here a range of examples.

6.1. The mean cluster size

Asymptotics for stationary series suggest that the mean cluster size–the number of days in a cold spell during which a very low temperature is reached–is approximately independent of the actual value of that low temperature. We therefore simulate the sample path of extreme events from the fitted model a large number of times, and take the sample mean cluster size as our estimator, with the monthly thresholds being taken as the level at which events are considered extreme. Thus, in this context, observations are only 'extreme' relative to 'typical' behaviour within that month.

Within the Markov model, the mean cluster size depends only on the choice of bivariate dependence model, in our case the logistic model. However, since the parameter of the fitted logistic model is time-dependent it follows that the mean cluster size will also vary throughout the year. For subsequent calculations it is necessary to evaluate the mean cluster size on a daily basis; for accuracy we used the exact procedure of Smith[5] in preference to simulation, with the logistic parameter taken as $\alpha(t_i)$; $i = 1, \ldots, 365$, respectively, where $t_i = i/365$, to obtain daily values,

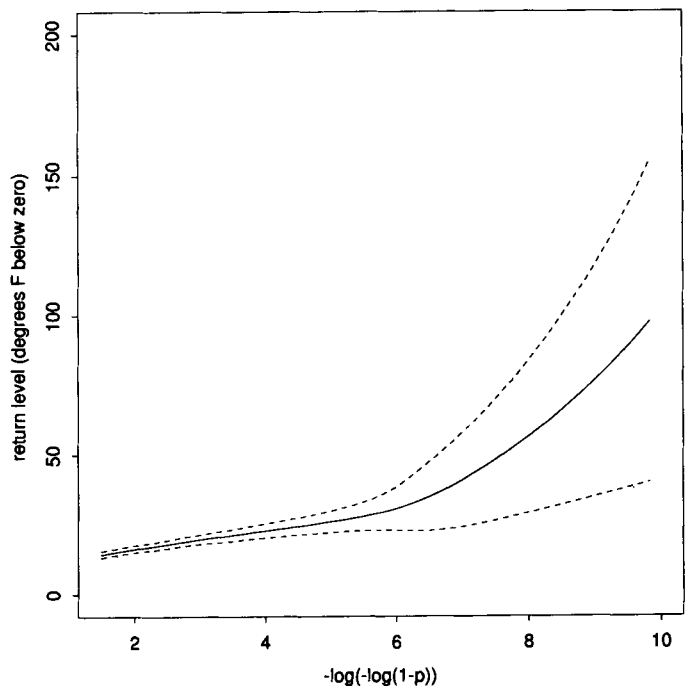

Figure 9. Return levels, y_p, of the annual minimum (continuous curve) and 95 per cent confidence intervals (dashed lines) obtained by the delta method. Estimates obtained using model 8

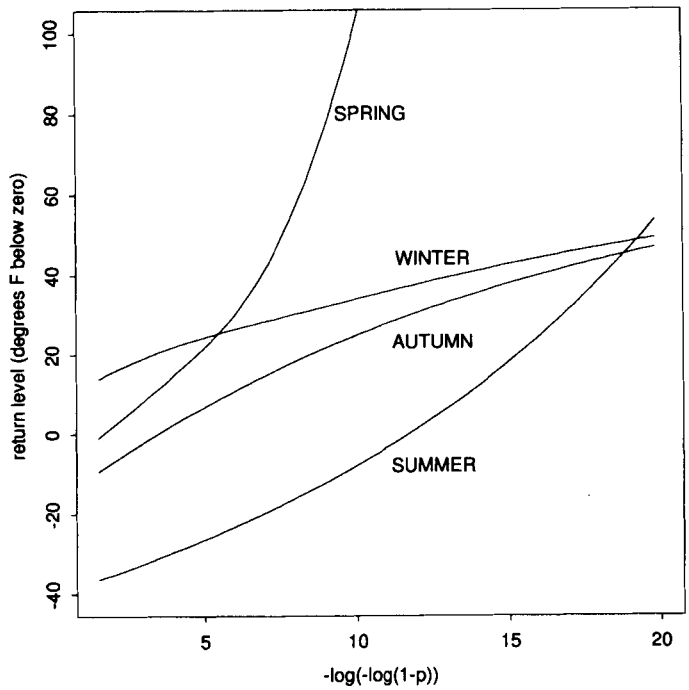

Figure 10. Return levels, y_p, of the seasonal minimum. Winter, spring, summer and autumn correspond to the months December–February, March–May, June–August and September–November, respectively. Estimates obtained using model 7

θ_i^{-1}. To illustrate the seasonal pattern, Table I gives the values of θ_i^{-1} based on the separate monthly values of α_i obtained from model 4. It is clear that the propensity of the extremes to cluster varies throughout the year.

6.2. Return levels

It is now possible to calculate the distribution function of the annual minimum return levels. Following Husler[10] this takes the form

$$G_I(y) = \prod_{i \in I} \Pr\{Y_i \leqslant y\}^{\theta_i}, \tag{7}$$

where $I = \{1, \ldots, 365\}$ indexes the daily series, and θ_i is the extremal index for day i. By restricting I to index days within a specified period only, we can also obtain the distribution function of the corresponding 'seasonal minimum'. The terms required in the product (7) are obtained directly from the fitted model, with the θ_i calculated as described in Section 6.1. In fact, it is usual to regard (7) as an equation for y given fixed $G_I(y)$, i.e. to solve $G_I(y_p) = 1 - p$ for some small $p > 0$. In this context, y_p is termed the return level associated with an exceedance probability of p. For a range of fixed values of p we therefore solve (7) to obtain y_p, and also obtain standard errors for y_p by use of the delta method. In the case of the annual minimum temperatures, these are plotted on the usual scale of $-\log[-\log(1-p)]$. Figures 8 and 9 show these plots for models 7 and 8, respectively. In each case the estimates are similar but model 8 gives wider confidence intervals as a consequence of the larger shape parameters in March

and April. The corresponding graphs giving the separate return level curves for each season are shown in Figure 10 and 11, respectively. In each case models 7 and 8 give remarkably similar results.

As expected, in Figures 10 and 11 the probabilities of severely cold temperatures are far higher in the winter and spring than for the other seasons. What is surprising though is that the 'spring' curve is dominant at extreme levels whichever model is considered. However, since $\xi(t)$ is positive only in the spring, this is the only period with an estimated infinite upper endpoint in its distribution, so this domination is inevitable at extreme levels. This feature is inconsistent with known meteorology, and thus illustrates the limitations of extrapolating the fitted model far beyond the range of the data.

6.3. Distribution of the last day of frost

For some agricultural applications, such as the scheduling of crop planting, it is of interest to know when the last pre-summer day of sub-freezing, or some other extremely low temperature, is likely to occur. We denote this day by D_F. A procedure to model the distribution of D_F is described by Husler;[11] here we adapt this procedure to allow for the temporal dependence in the extremes and non-stationarity as estimated through models 7 and 8. Our model therefore provides the first opportunity to examine the distribution of D_F in a way which is consistent with asymptotic models for the extremes themselves.

We use the fitted models 7 and 8 to calculate the distribution function of the last occurrence of any specified low level as follows. Let $-t_c$ be some critically low temperature, and let D_F denote

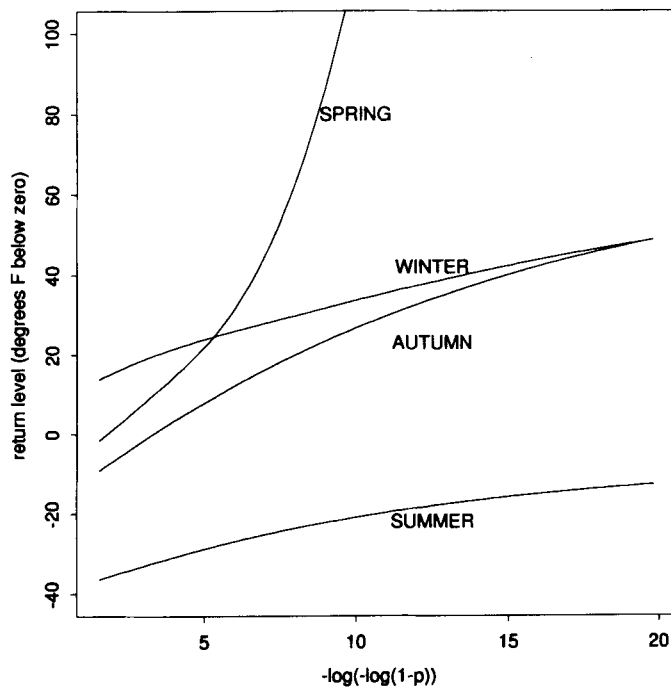

Figure 11. Return levels, y_p, of the seasonal minimum. Winter, spring, summer and autumn correspond to the months December–February, March–May, June–August and September–November, respectively. Estimates obtained using model 8

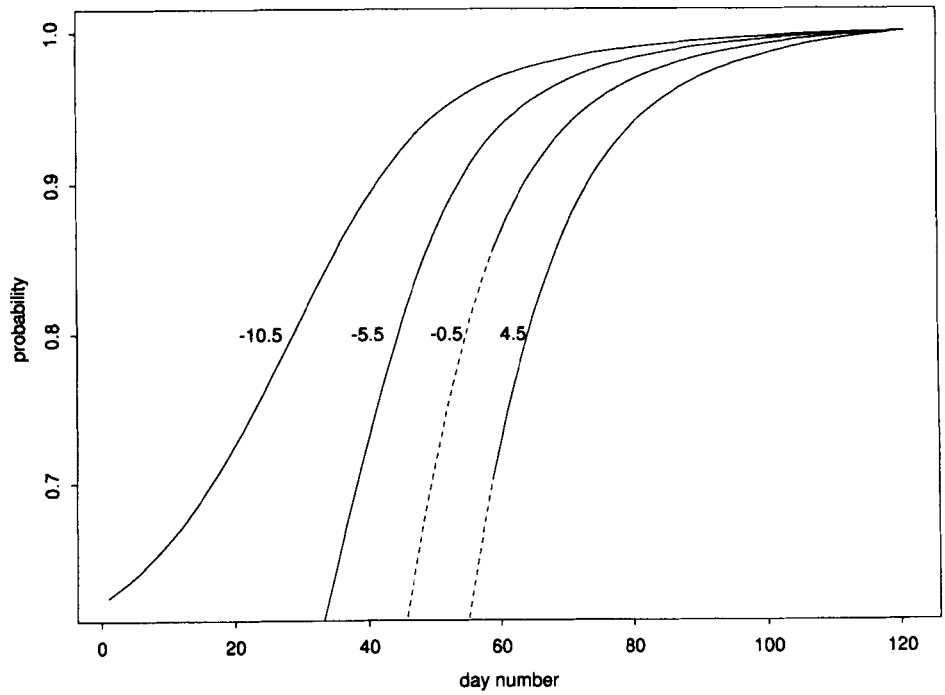

Figure 12. Distribution function of the last occurrence, until the next winter cycle, of specified low temperatures t_c = 10·5, 5·5, 0·5, −4·5°F. Estimates obtained using model 8

the last day the temperature falls below $-t_c$. Then

$$\Pr\{D_F \leqslant d\} = \prod_{i \in J_d} \Pr\{Y_i \leqslant t_c\}^{\theta_i}, \tag{8}$$

where $J_d = \{d+1, \ldots d_e\}$ with d_e denoting the day after which temperatures below $-t_c$ are regarded as implausible until the next winter cycle. Thus, the distribution function (8) has an identical structure to that of (7), the only difference being in the indexing set. Figure 12 illustrates the distribution function for various choices of $-t_c$ using model 8 only. The results using model 7 are almost completely identical. One slight complication in this procedure is that strictly we have a model for $\Pr\{Y_i \leqslant t_c\}$ only when t_c is above the relevant threshold for day i. It is possible that a particular choice of t_c falls below the specified threshold over a range of the days indexed by J_d. In our example this happened for the choices $t_c = -0{\cdot}5$ and 4·5°F. An approximation in this case is to replace the appropriate terms $\Pr\{Y_i \leqslant t_c\}$ by terms obtained by extrapolating the fitted generalized Pareto distributional tail model back into the bulk of the distribution. Applying this procedure led to the dashed portion of the curve in Figure 12, which seems a reasonable extrapolation of the remainder of that curve.

6.4. Other examples

There are many other practical questions of interest concerning temporal aspects of the low-temperature process which can be formulated in terms of functionals of within-cluster observations. All such aspects can be estimated using procedures similar to the above. In the stationary

analysis of Smith *et al.*,[2] a number of other examples are considered. These include: the mean number of downcrossings of a particular low level; the cluster aggregate distribution, where a cluster aggregate is defined as the sum of the terms $(Y_i - t_l)_+$ within a cluster, for some level t_l; and the distribution of the number of cold waves in a year, where a cold wave is deemed to have occurred if there are a specified number of consecutive days during which the temperature stays below a certain level. At the expense of additional computing resources, these characteristics can also be estimated within the framework of the seasonal model. This is achieved by simulating the distribution of the appropriate intra-cluster statistic for each set of daily parameters $(\mu(t_i), \sigma(t_i), \xi(t_i), \alpha(t_i))$; $i = 1, \ldots, 365$. Combining this estimate with the Poisson process model for occurrences of clusters enables the distribution of the corresponding *annual* characteristic to be estimated (see Theorem 1 of Smith *et al.*[2]).

ACKNOWLEDGEMENTS

We are grateful to Peter Diggle for some modelling suggestions and to Thomas Karl of the National Climate Data Center for the temperature data. R.L.S. was partially supported by the NSF. J.A.T. and S.G.C. were each partly funded by a Nuffield Foundation grant and the analysis used equipment provided by the SERC under the Complex Stochastic Systems Initiative.

REFERENCES

1. Leadbetter, M. R., Lindgren, G. and Rootzén, H. *Extremes and Related Properties of Random Sequences and Series*, Springer Verlag, New York, 1983.
2. Smith, R. L., Tawn, J. A. and Coles, S. G. 'Markov chain models for threshold exceedances', Submitted, 1993.
3. Cox, D. R. 'Statistical analysis of time series, some recent developments', *Scandinavian Journal of Statistics*, **8,** 93–115 (1981).
4. Leadbetter, M. R. 'Extremes and local dependence in stationary sequences', *Zeitshrift Wahrscheinlichkeitstheone und Gebiete*, **65,** 291–306 (1983).
5. Smith, R. L. 'The extremal index for a Markov chain', *Journal of Applied Probability*, **29,** 37–45 (1982).
6. Smith, R. L. 'Extreme value analysis of environmental time series: an application to trend detection in ground level ozone', *Statistical Science*, **4,** 367–393 (1989).
7. Barrett, J. H. 'An extreme value analysis of the flow of Burbage Brook', *Stochastic Hydrology and Hydrolics*, **6,** 151–165 (1992).
8. Davison, A. C. and Smith, R. L. 'Models for exceedances over high thresholds (with discussion)', *Journal of the Royal Statistical Society, Series B*, **52,** 393–442 (1990).
9. Barnett, V. and Lewis, T. 'A study of low-temperature probabilities in the context of an industrial problem (with discussion)', *Journal of the Royal Statistical Society, Series A*, **130,** 177–206 (1967).
10. Husler, J. 'Extreme values of non-stationary random sequences', *Journal of Applied Probability*, **23,** 937–950 (1986).
11. Husler, J. 'Frost data: a case study on extreme values of non-stationary sequences', *in* Tiago de Oliveira, J. (ed.), *Statistical Extremes and Applications*, pp. 513–520 (1984).